Supplemental Data

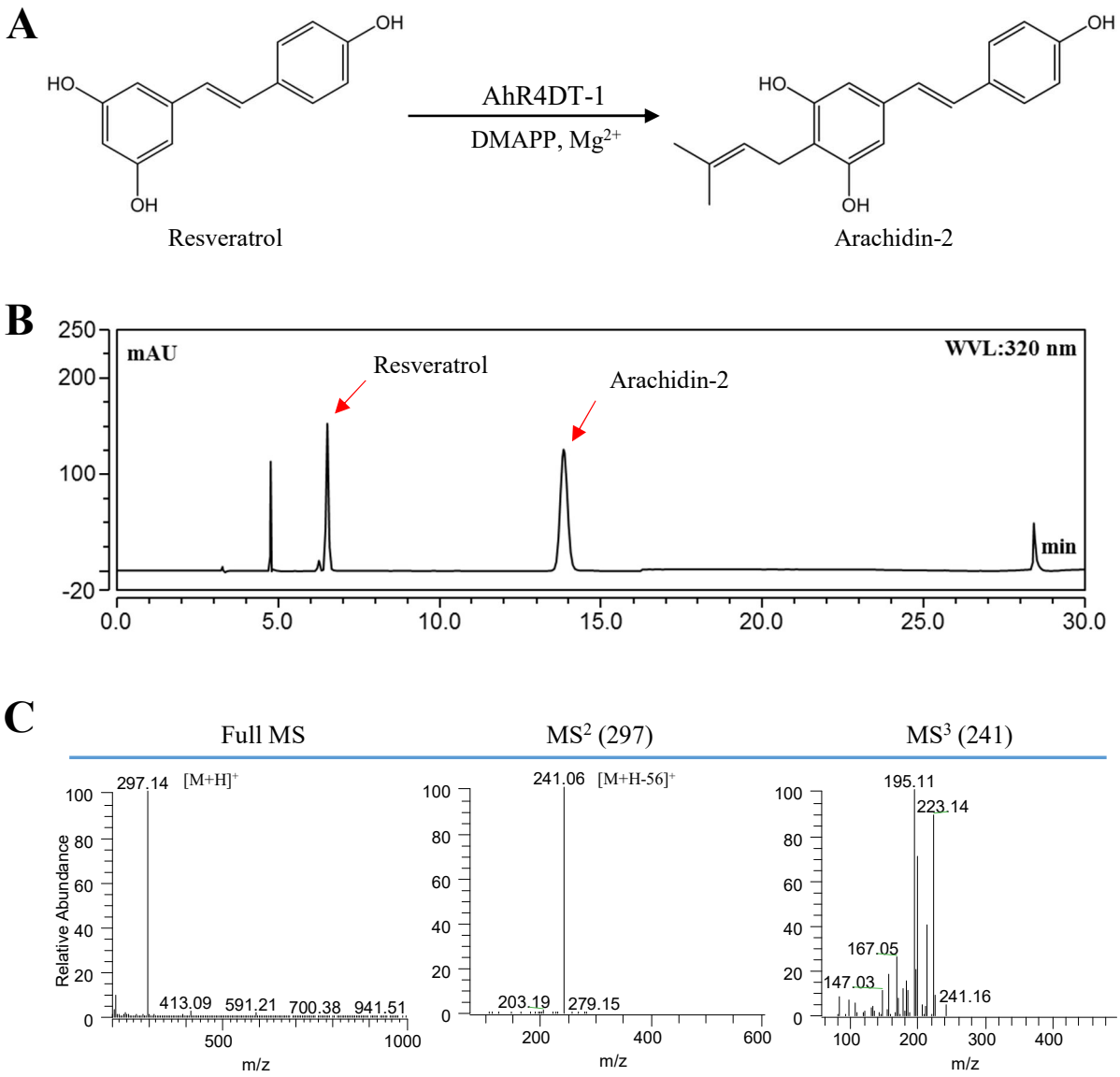

Figure S1. Prenylation of resveratrol by AhR4DT-1.

Prenylation activity of AhR4DT-1 in microsomal fraction of *Nicotiana benthamiana* leaf after vacuum infiltration with *Agrobacterium tumefaciens* LBA4404 harboring pBIB-Kan-AhR4DT-1.

(A) Chemical structures of resveratrol and its prenylated product, arachidin-2.

(B) HPLC chromatograms (UV 320 nm) of ethyl acetate extraction of reaction mixtures contained 100 µM resveratrol, 300 µM DMAPP, 10 mM $MgCl_2$, 5 mM DTT and 30 µg microsomal fraction in a pH 9.0 Tris-HCl buffer for 40 min.

(C) HPLC-PAD-ESI-MS^3 analysis of prenylated product, arachidin-2.

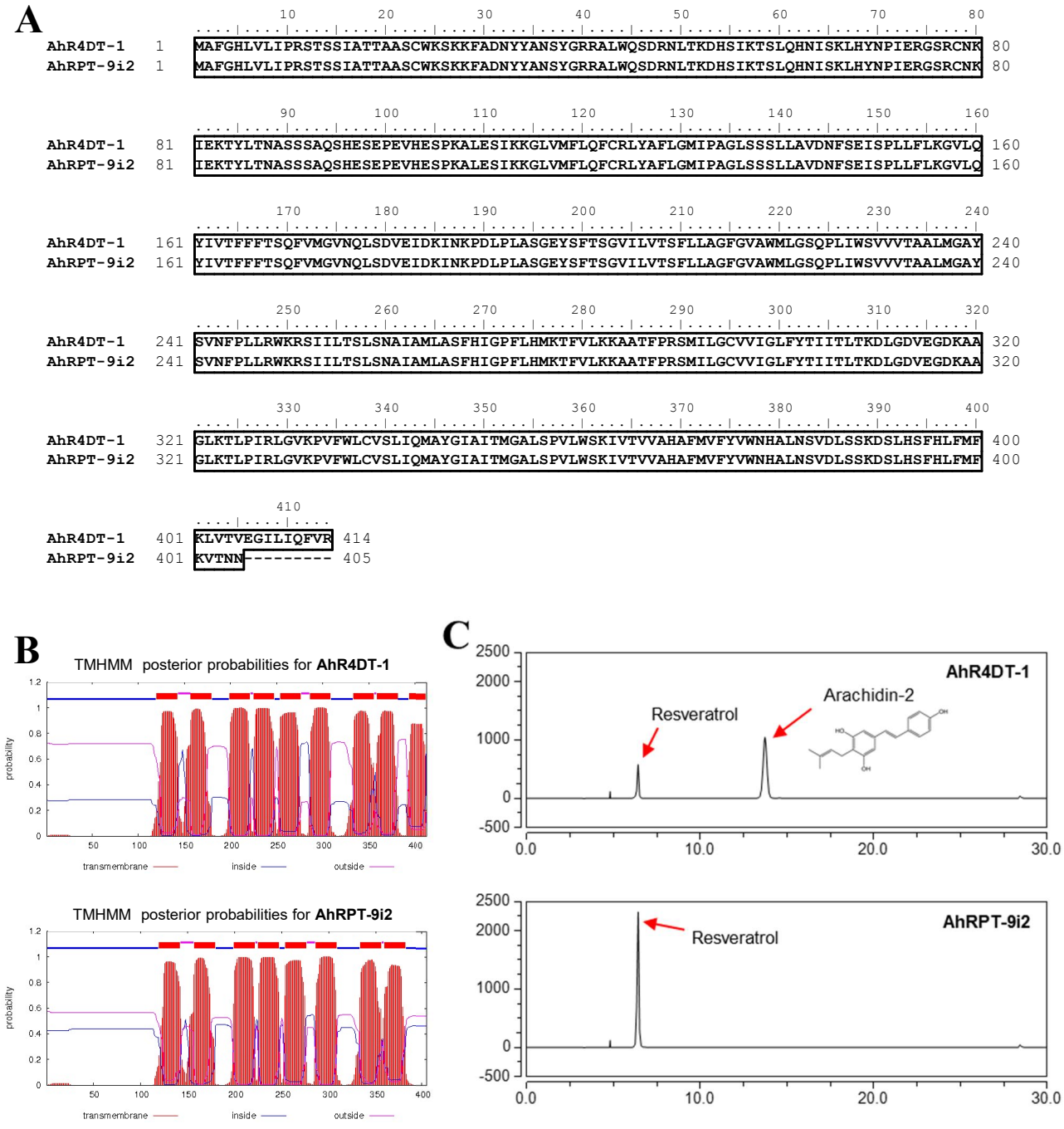

Figure S2. Comparison of AhR4DT-1 and AhRPT-9i2.

(A) Alignment of AhR4DT-1 with AhRPT-9i2 was performed using ClustalX.

(B) Potential transmembrane domains of AhR4DT-1 and AhRPT-9i2 were predicted by TMHMM.

(C) Resveratrol prenylation activity of AhR4DT-1 and AhRPT-9i2 were analyzed by using HPLC.

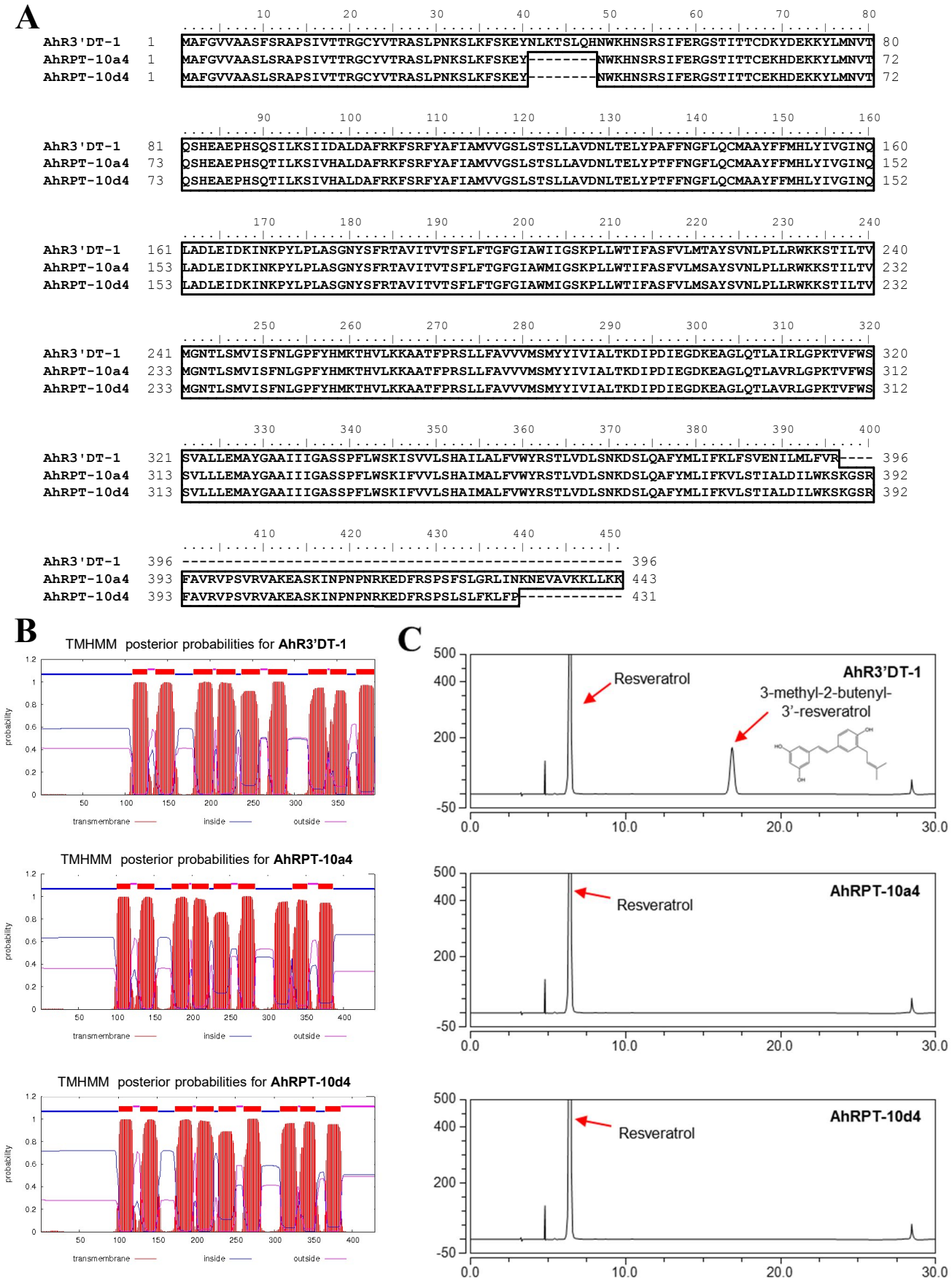

Figure S3. Comparison of AhR3'DT-1, AhRPT-10a4 and AhRPT-10d4.

(A) Alignment of AhR3'DT-1, AhRPT-10a4 and AhRPT-10d4 was performed using ClustalX.

(B) Potential transmembrane domains of AhR3'DT-1, AhRPT-10a4 and AhRPT-10d4 were predicted by TMHMM.

(C) Resveratrol prenylation activity of AhR3'DT-1, AhRPT-10a4 and AhRPT-10d4 were analyzed by using HPLC.

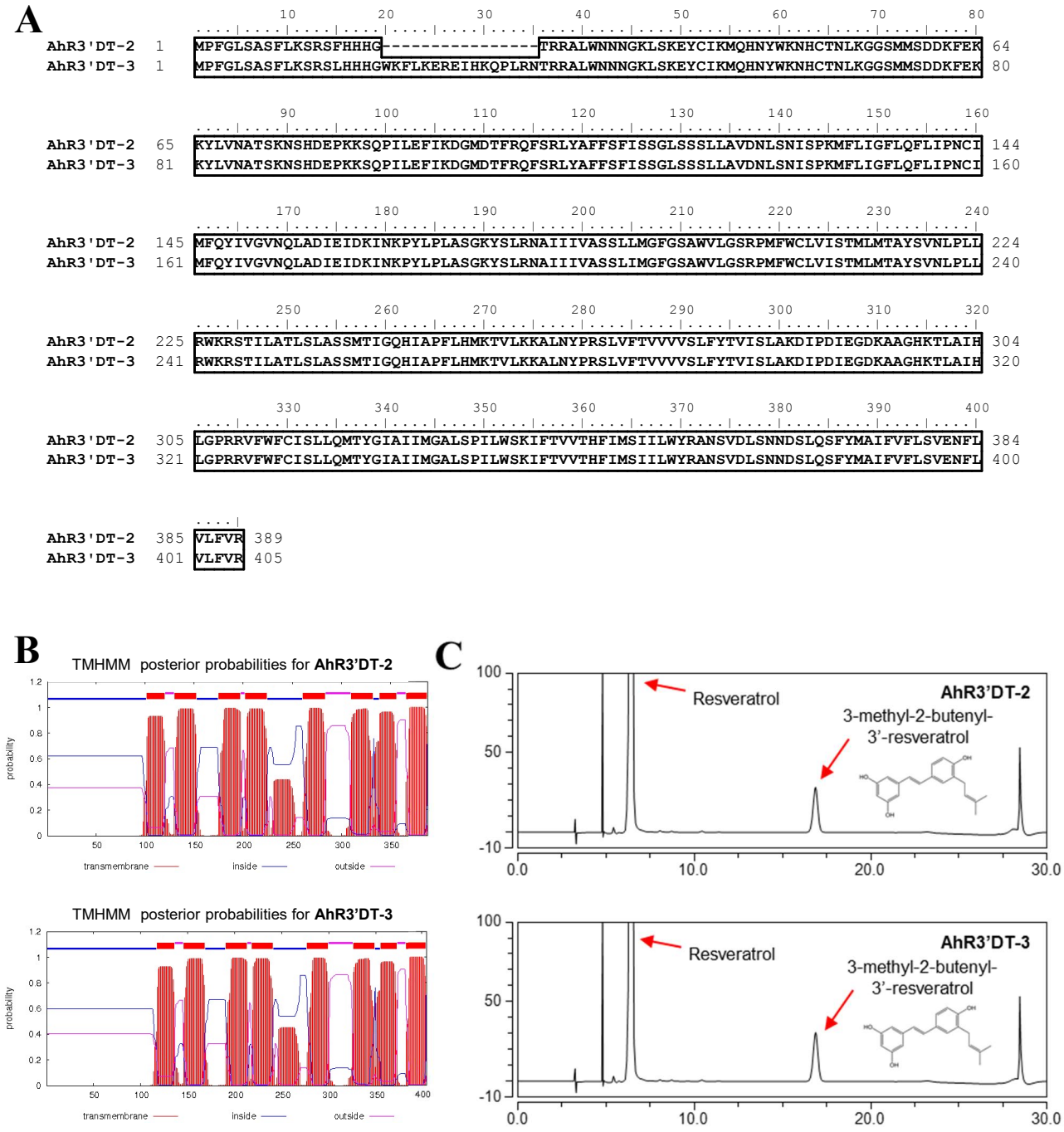

Figure S4. Comparison of AhR3'DT-2 and AhR3'DT-3.

(A) Alignment of AhR3'DT-2 with AhR3'DT-3 was performed using ClustalX.

(B) Potential transmembrane domains of AhR3'DT-2 and AhR3'DT-3 were predicted by TMHMM.

(C) Resveratrol prenylation activity of AhR3'DT-2 and AhR3'DT-3 were analyzed by using HPLC.

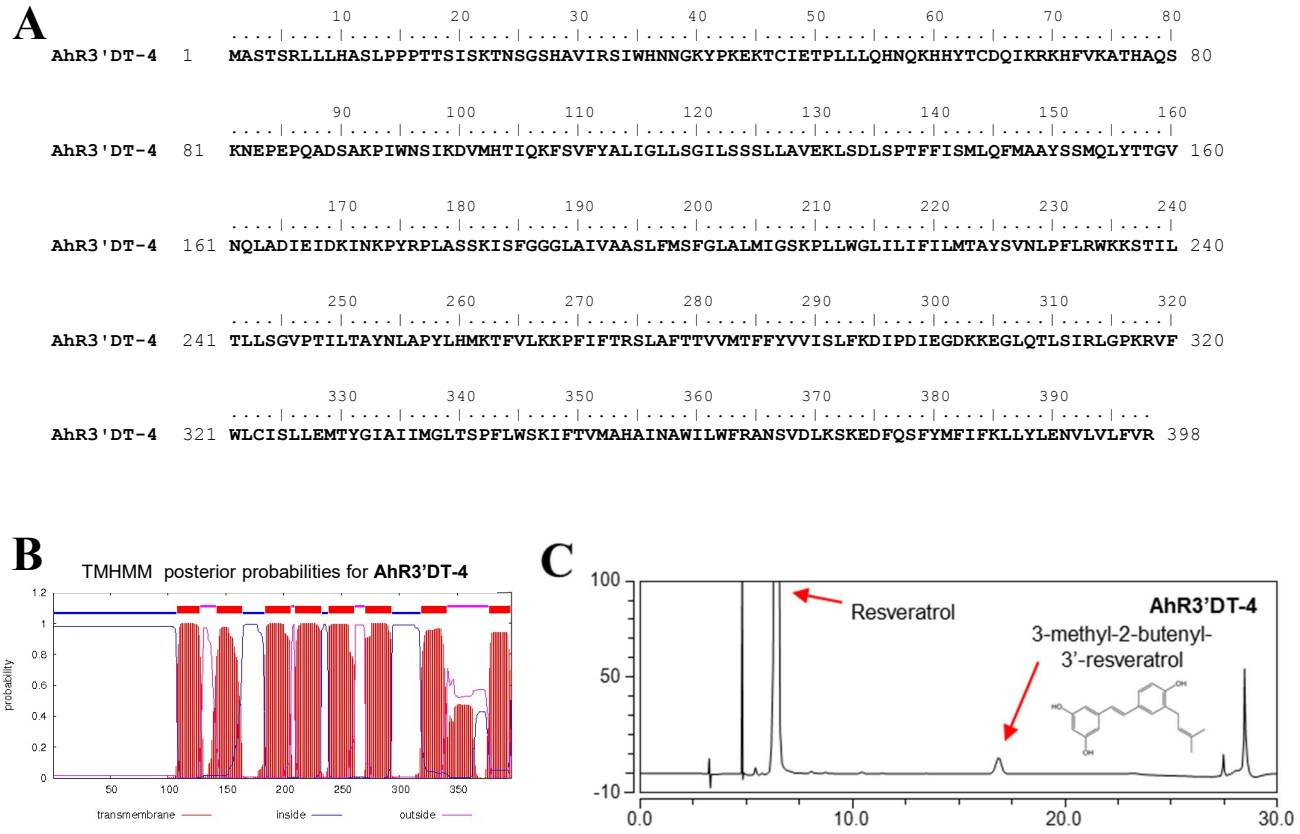

Figure S5. Structural analysis of AhR3'DT-4.
(A) Primary structure of AhR3'DT-4.
(B) Potential transmembrane domains of AhR3'DT-4 was predicted by TMHMM.
(C) Resveratrol prenylation activity of AhR3'DT-4 was analyzed by using HPLC.

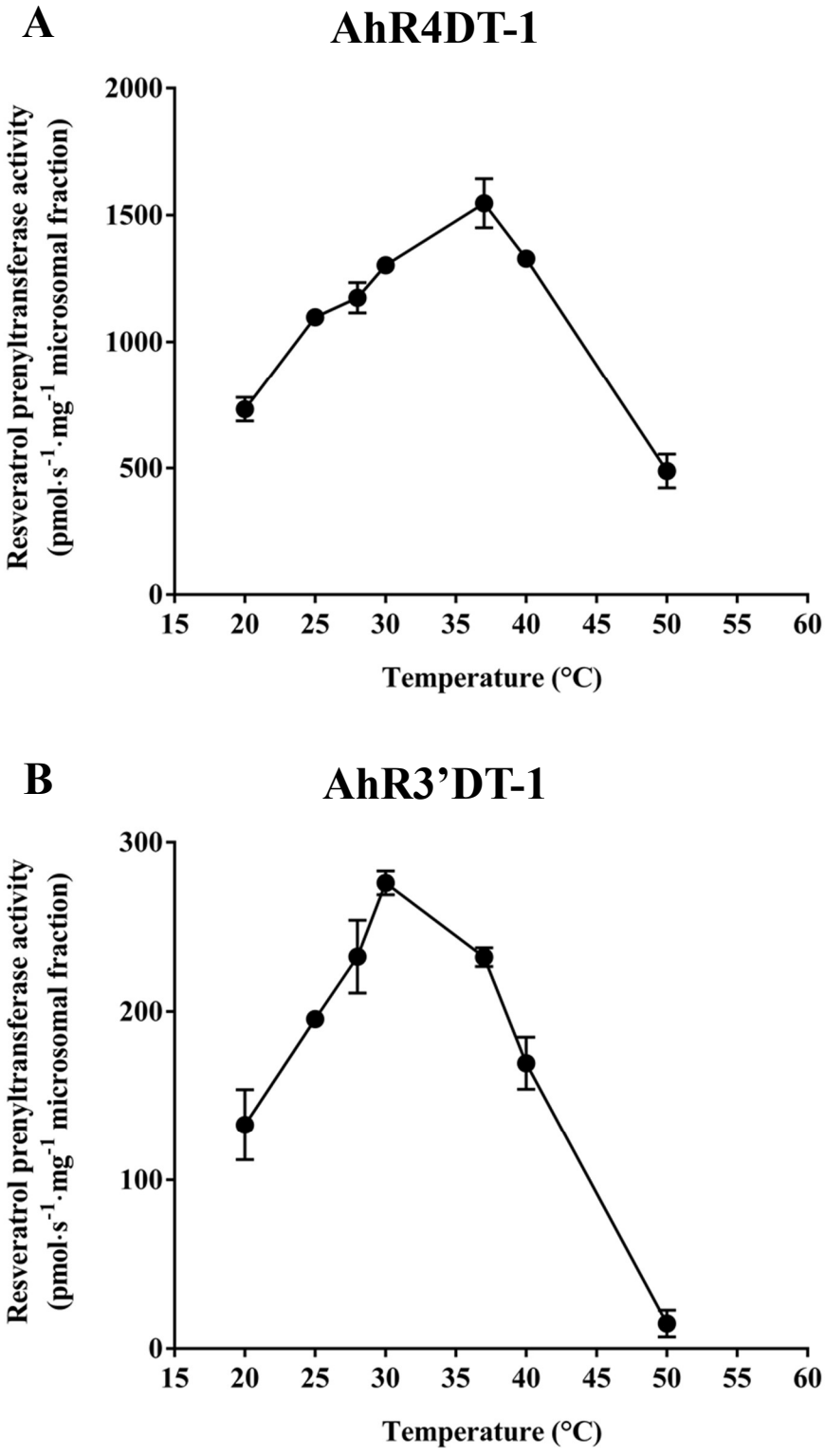

Figure S6. Temperature dependency of AhR4DT-1 and AhR3'DT-1 activity. AhR4DT-1 (A) and AhR3'DT-1 (B) activities were measured at various temperature (20, 25, 28, 30, 37, 40 and 50 ºC) in 100 mM Tris-HCl buffer (pH 9.0) for 40 mins.

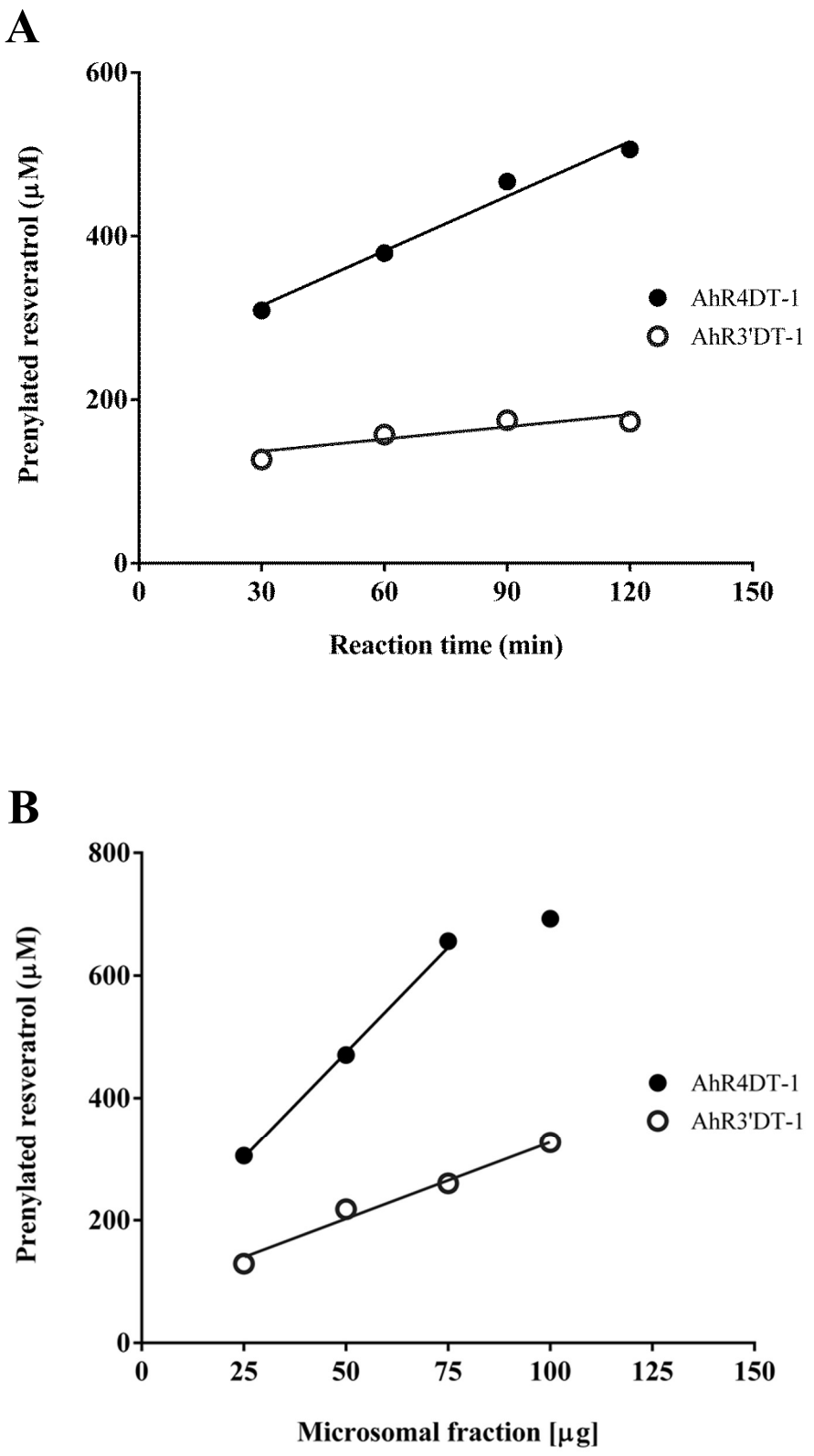

Figure S7. Resveratrol prenylation activity of AhR4DT-1 and AhR3'DT-1.
(A) Concentrations of generated prenylated resveratrol from AhR4DT-1 and AhR3'DT-1 reaction mixtures with varying incubation times (30, 60, 90 and 120 min) were quantified by HPLC.
(B) Concentrations of generated prenylated resveratrol from AhR4DT-1 and AhR3'DT-1 reaction mixtures with varying amounts of microsomal fraction (25, 50, 75 and 100 µg) were quantified by HPLC.

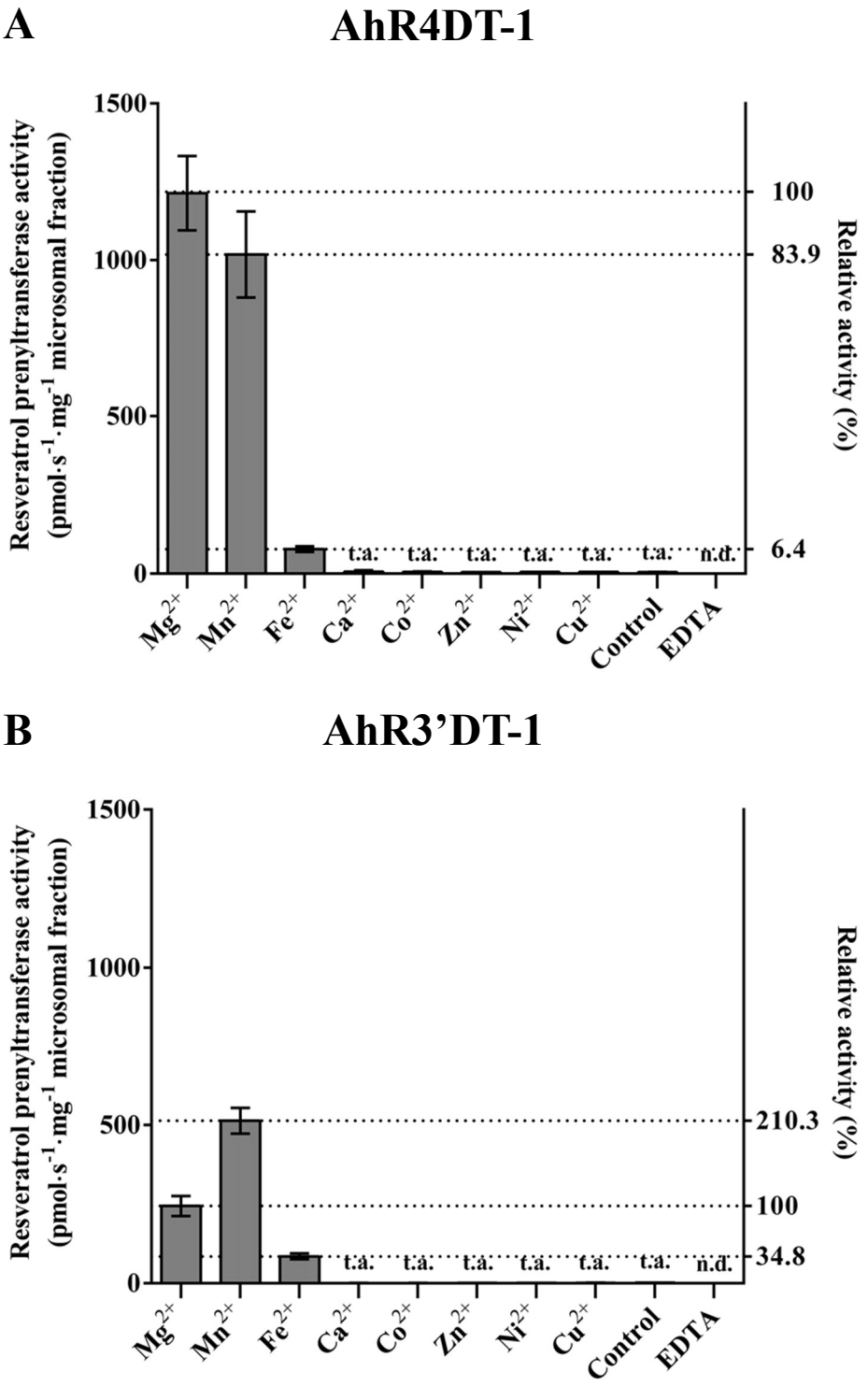

Figure S8. Divalent cation dependency of AhR4DT-1 and AhR3'DT-1 activity.
AhR4DT-1 (A) and AhR3'DT-1 (B) activity with various divalent cation were measured with 10 mM $MnCl_2$, $FeCl_2$, $CaCl_2$, $CoCl_2$, ZnCl2, $NiCl_2$, or $CuCl_2$ and the enzyme activity was compared with the reaction of 10 mM $MgCl_2$. Reactions without divalent cation and 10 mM EDTA instead of $MgCl_2$ were used as controls. All the reactions were performed in 100 mM Tris-HCl buffer (pH 9.0) at 28 ºC for 40 min. (t.a., trace amount (<0.5%), n.d., Not detected.). Means and the standard deviation (error bars) were calculated from three replicates.

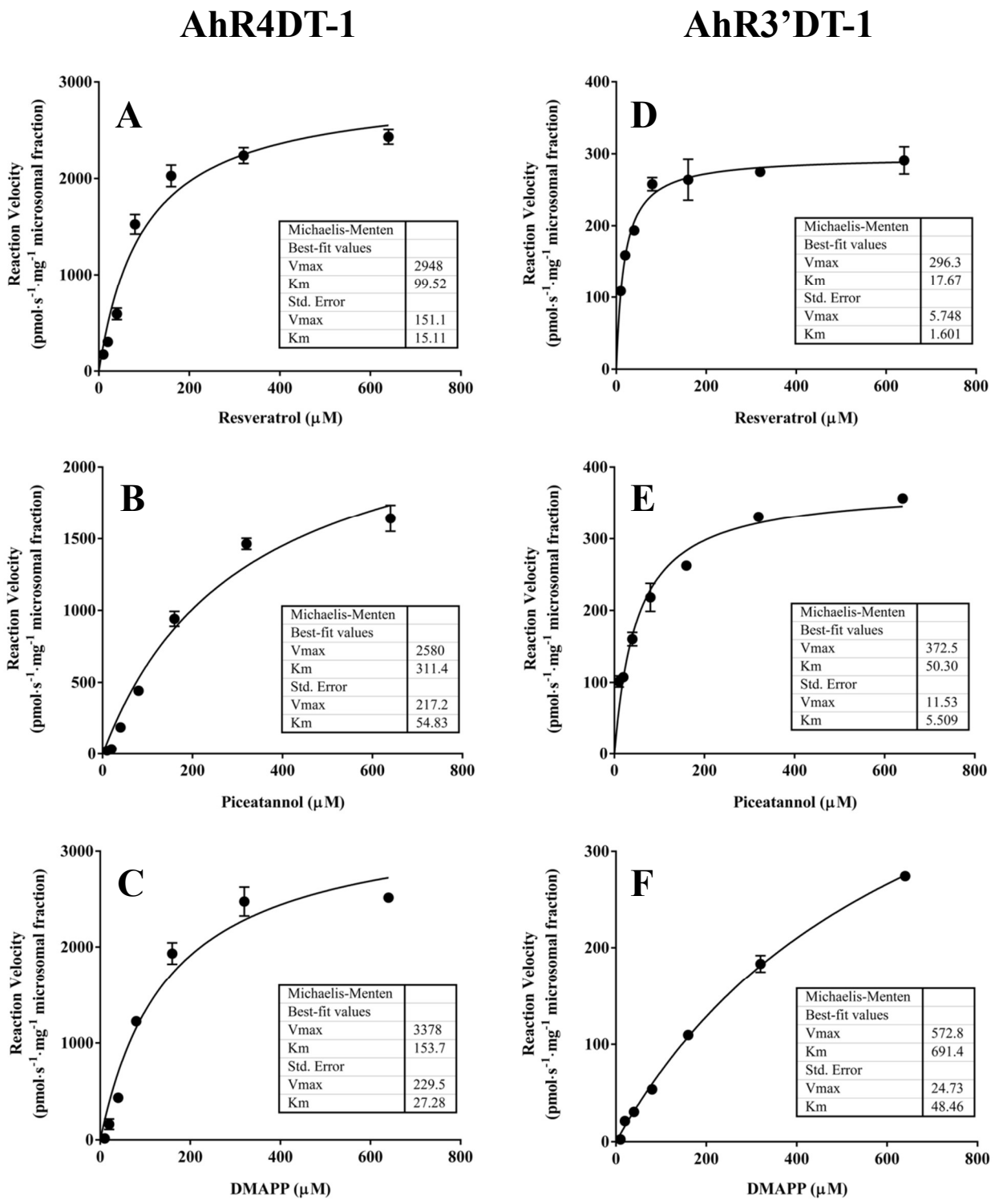

Figure S9. Kinetic values of AhR4DT-1 and AhR3'DT-1.
Dependency of AhR4DT-1 (left) and AhR3'DT-1 (right) on the concentration of resveratrol (A&D), piceatannol (B&E) and DMAPP (C&F) measured with a microsomal fraction from leaves of *Nicotiana benthamiana*. The apparent K_m and V_{max} values for resveratrol and piceatannol were determined with varying concentrations (10~640 μM) using 640 μM DMAPP as prenyl donor, while that for DMAPP were determined with varying concentrations (10~640 μM) using 640 μM resveratrol as prenyl acceptor. All the values were calculated from nonlinear regression analysis with Michaelis-Menten equation by Graphpad Prism 6 software. Means and the standard deviation (error bars) were calculated from three replicates.

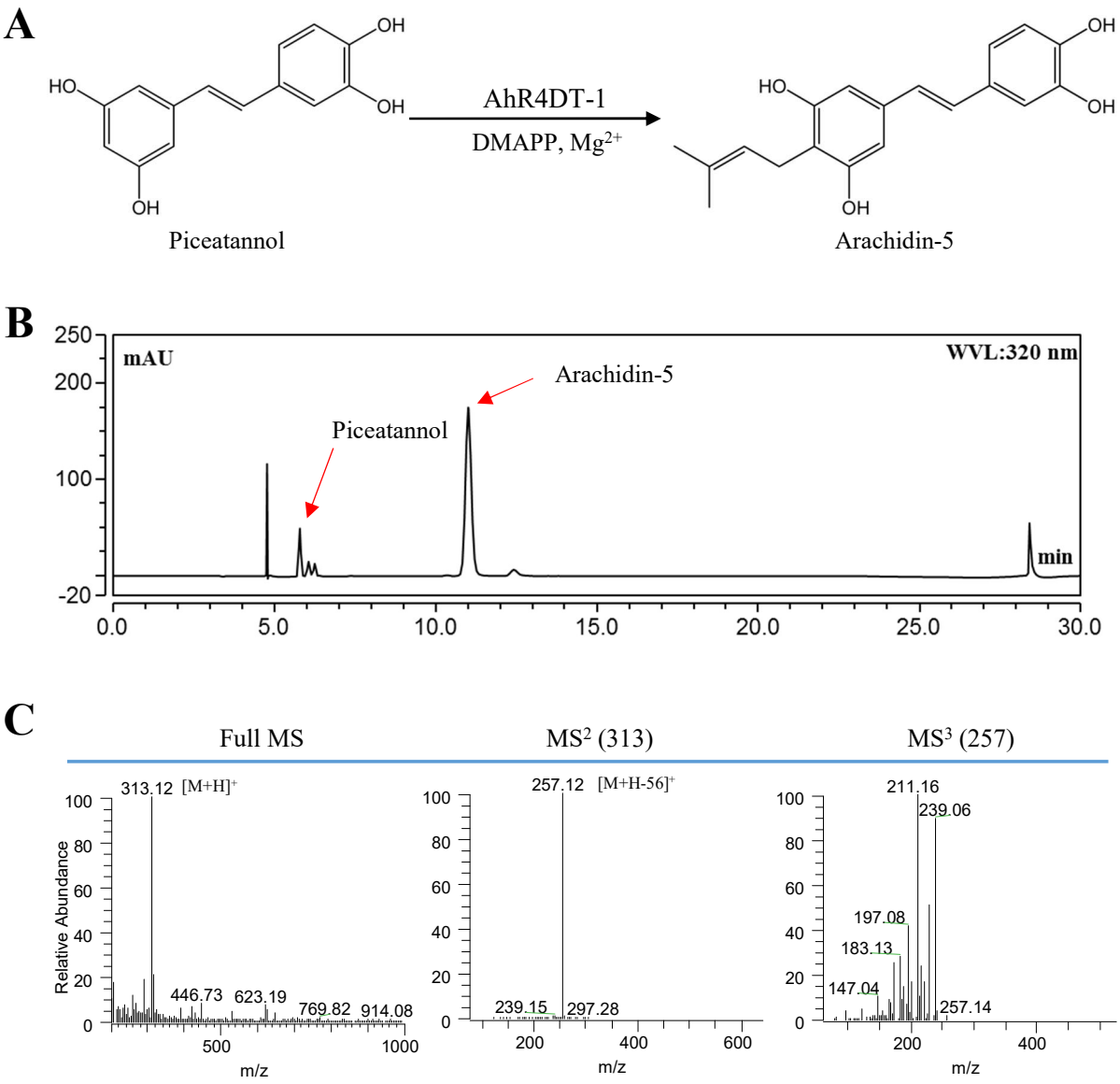

Figure S10. Prenylation of piceatannol by AhR4DT-1.
Substrate specificity of AhR4DT-1 in microsomal fraction of *Nicotiana benthamiana* leaf after vacuum infiltration with *Agrobacterium tumefaciens* LBA4404 harboring pBIB-Kan-AhR4DT-1.
(A) Chemical structures of piceatannol and its prenylated product.
(B) HPLC chromatograms (UV 320 nm) of ethyl acetate extraction of reaction mixtures contained 100 µM piceatannol, 300 µM DMAPP, 10 mM $MgCl_2$, 5 mM DTT and 30 µg microsomal fraction in a pH 9.0 Tris-HCl buffer for 40 min.
(C) HPLC-PAD-ESI-MS^3 analysis of prenylated product, arachidin-5.

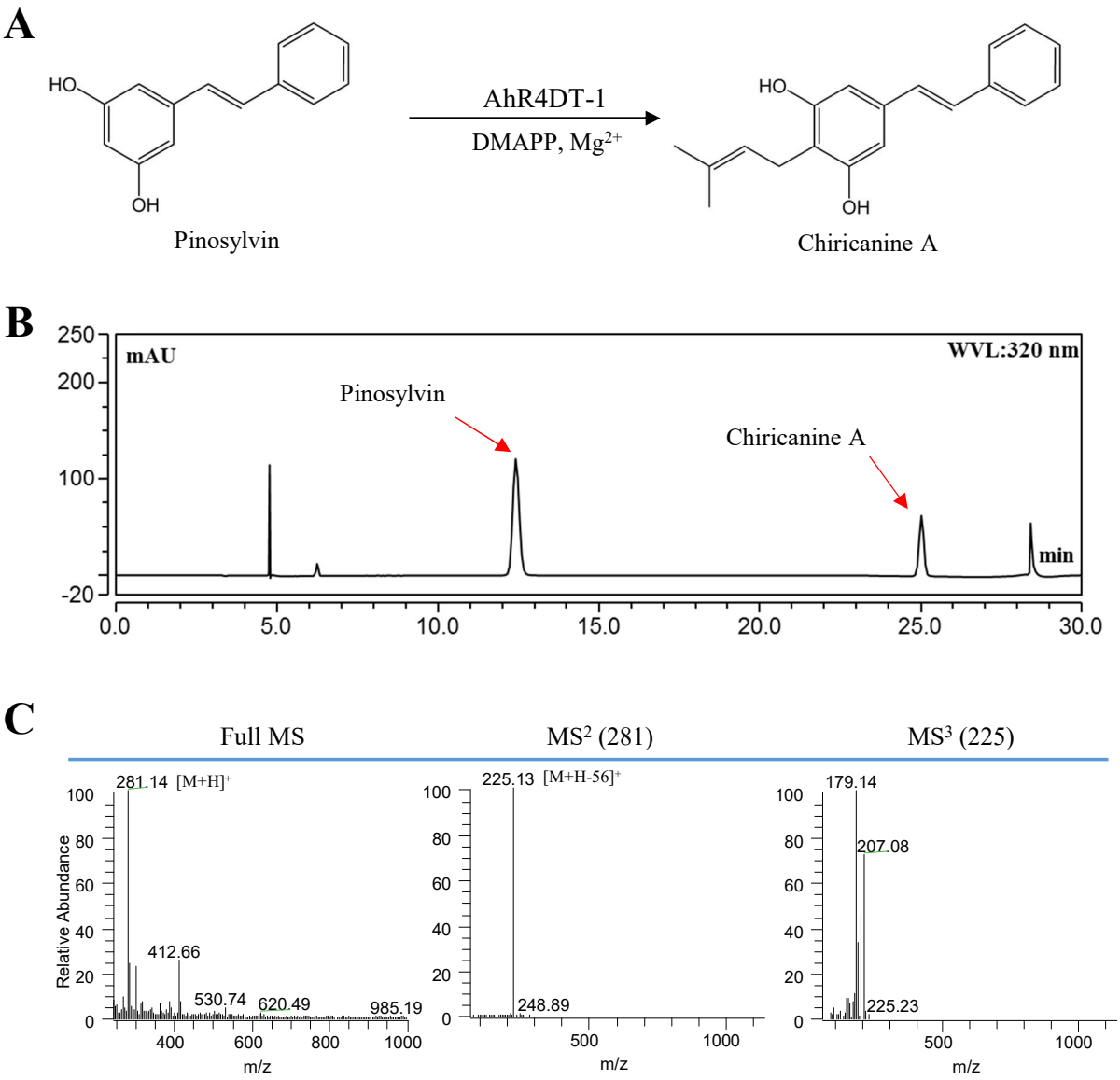

Figure S11. Prenylation of pinosylvin by AhR4DT-1.
Substrate specificity of AhR4DT-1 in microsomal fraction of *Nicotiana benthamiana* leaf after vacuum infiltration with *Agrobacterium tumefaciens* LBA4404 harboring pBIB-Kan-AhR4DT-1.
(A) Chemical structures of pimosylvin and its prenylated product.
(B) HPLC chromatograms (UV 320 nm) of ethyl acetate extraction of reaction mixtures contained 100 µM pinosylvin, 300 µM DMAPP, 10 mM $MgCl_2$, 5 mM DTT and 30 µg microsomal fraction in a pH 9.0 Tris-HCl buffer for 40 min.
(C) HPLC-PAD-ESI-MS^3 analysis of prenylated product, chiricanine A.

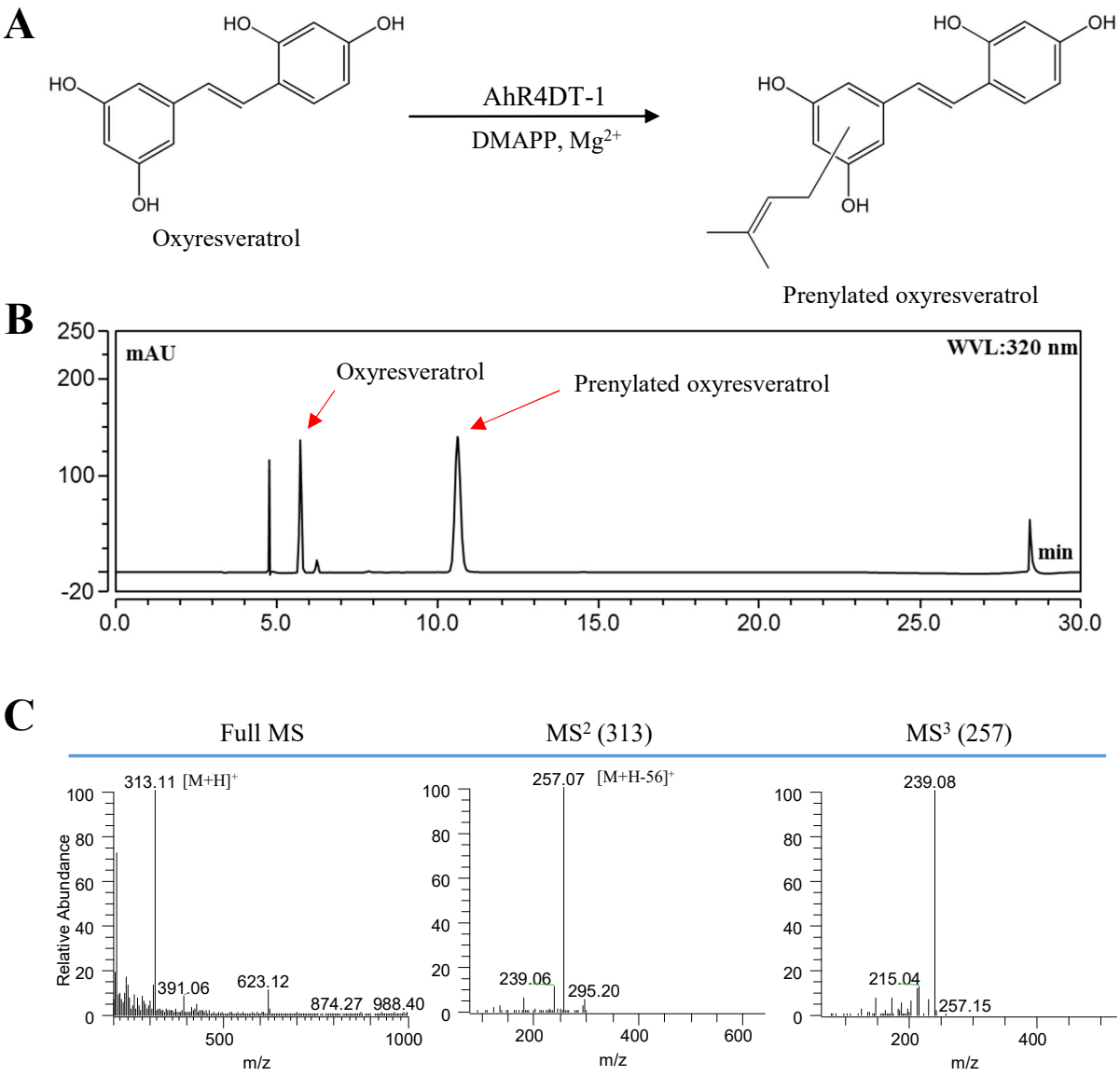

Figure S12. Prenylation of oxyresveratrol by AhR4DT-1.
Substrate specificity of AhR4DT-1 in microsomal fraction of *Nicotiana benthamiana* leaf after vacuum infiltration with *Agrobacterium tumefaciens* LBA4404 harboring pBIB-Kan-AhR4DT-1.
(A) Chemical structures of oxyresveratrol and its prenylated product.
(B) HPLC chromatograms (UV 320 nm) of ethyl acetate extraction of reaction mixtures contained 100 µM oxyresveratrol, 300 µM DMAPP, 10 mM $MgCl_2$, 5 mM DTT and 30 µg microsomal fraction in a pH 9.0 Tris-HCl buffer for 40 min.
(C) HPLC-PAD-ESI-MS^3 analysis of prenylated product.

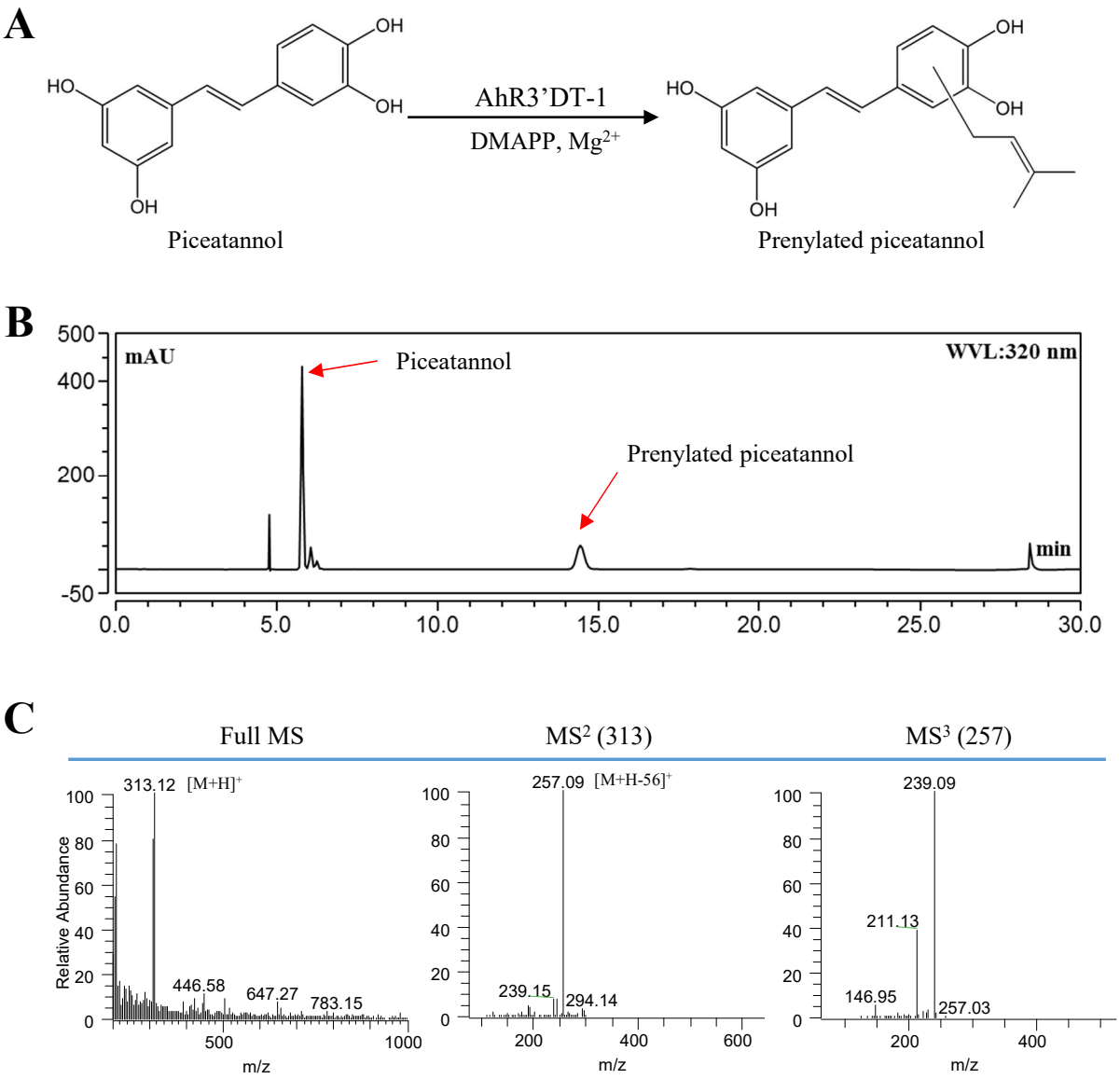

Figure S13. Prenylation of piceatannol by AhR3'DT-1.
Substrate specificity of AhR3'DT-1 in microsomal fraction of *Nicotiana benthamiana* leaf after vacuum infiltration with *Agrobacterium tumefaciens* LBA4404 harboring pBIB-Kan-AhR3'DT-1.
(A) Chemical structures of piceatannol and its prenylated product.
(B) HPLC chromatograms (UV 320 nm) of ethyl acetate extraction of reaction mixtures contained 100 µM piceatannol, 300 µM DMAPP, 10 mM $MgCl_2$, 5 mM DTT and 30 µg microsomal fraction in a pH 9.0 Tris-HCl buffer for 40 min.
(C) HPLC-PAD-ESI-MS^3 analysis of prenylated product.

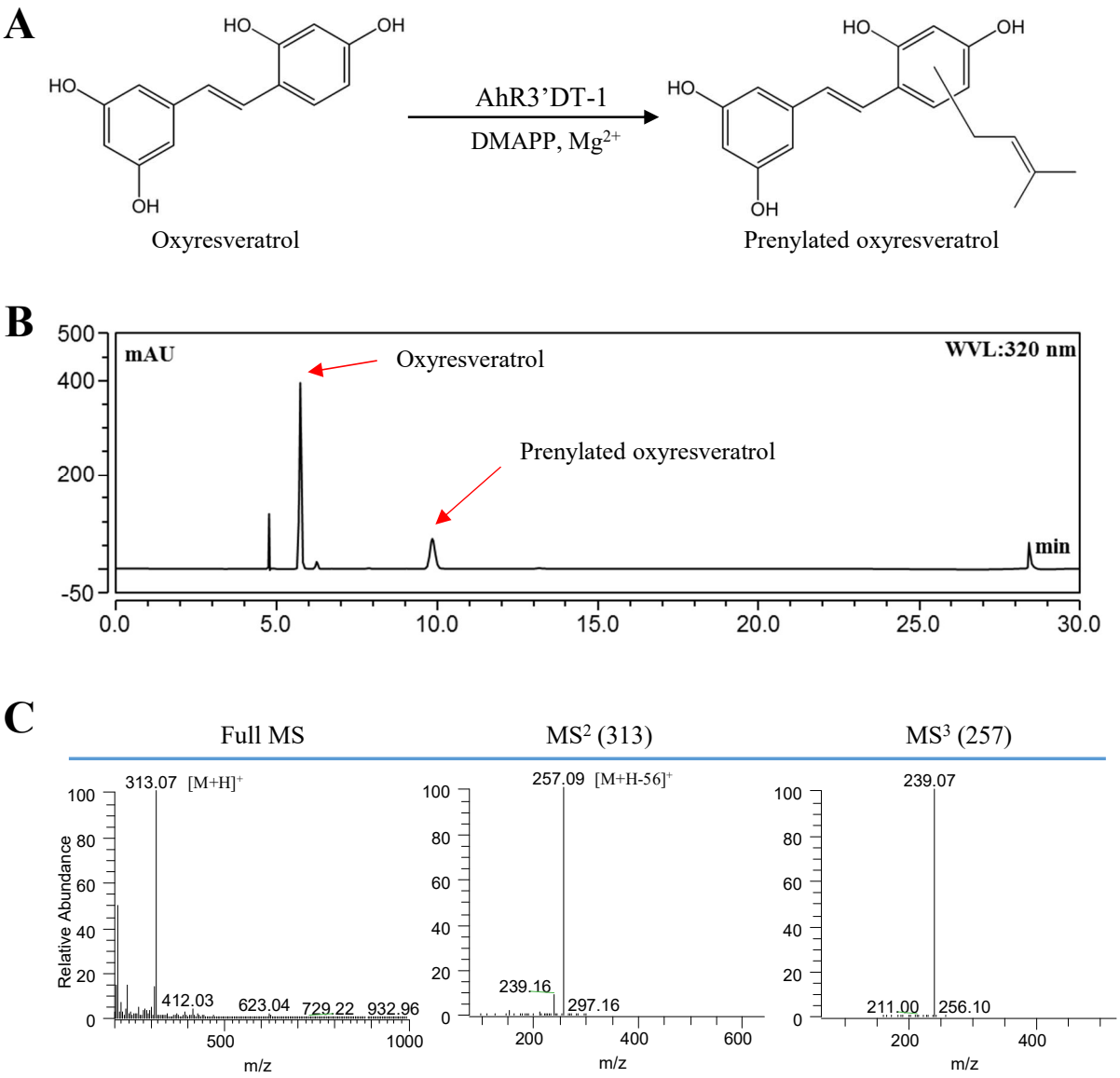

Figure S14. Prenylation of oxyresveratrol by AhR3'DT-1.
Substrate specificity of AhR3'DT-1 in microsomal fraction of *Nicotiana benthamiana* leaf after vacuum infiltration with *Agrobacterium tumefaciens* LBA4404 harboring pBIB-Kan-AhR3'DT-1.
(A) Chemical structures of oxyresveratrol and its prenylated product.
(B) HPLC chromatograms (UV 320 nm) of ethyl acetate extraction of reaction mixtures contained 100 µM oxyresveratrol, 300 µM DMAPP, 10 mM $MgCl_2$, 5 mM DTT and 30 µg microsomal fraction in a pH 9.0 Tris-HCl buffer for 40 min.
(C) HPLC-PAD-ESI-MS^3 analysis of prenylated product.

Table S1. List of primers used in this study.

The restriction site on each primer is underlined.

Name	Sequence (5'-3')	Reference
First screening for prenyltransferase gene		
PT-10-FW-*Not*I	TAGCGGCCGCATGGCTTTTGGTGTTGTTGCTGC	This study
PT-a-RV-*Kpn*I	ATCGATGGTACCCTATTTTTTAAGAAGTTTTTTTACTGC	This study
PT-d-RV-*Kpn*I	ATCGATGAGGTACCTCATGGAAATAGTTTGAACAGAGAG	This study
PT-k-RV-*Kpn*I	CGATGGTACCTCATCTAACAAAAAGCATAAGAATATTTTC	This study
Second screening for prenyltransferase gene		
PT-4-FW-*Not*I	TAGCGGCCGCATGCCTTTCGGACTCTCCGC	This study
PT-5-FW-*Not*I	TAGCGGCCGCATGGCTTCCACTTCCAGGCT	This study
PT-6-FW-*Not*I	TAGCGGCCGCATGGCTTTTAGGCTTCTAGGATC	This study
PT-9-FW-*Not*I	TAGCGGCCGCATGGCTTTTGGGCATTTGGTGT	This study
PT-b-RV-*Kpn*I	CTGAGGTACCTCAACGAACAAATTGTATAAGGATG	This study
PT-c-RV-*Kpn*I	CTGAGGTACCCTATCTCACGAAAAGTATAAGGATG	This study
PT-e-RV-*Kpn*I	CTGAGGTACCTCATCGAACAAAAAGTACAAGGAAG	This study
PT-i-RV-*Kpn*I	CTGAGGTACCTTAGTTATTGGTTACCTTAAACATA	This study
PT-m-RV-*Kpn*I	CTGAGGTACCTTATCTCACAAAAAGCACAAGGACA	This study
Promoter cloning		
Ca35S-FW-*Sal*I-1	ATCGATGTCGACAAGCTTGCATGCCTG	This study
TEV-RW-*Not*I	ATCGATGCGGCCGCGCTATCGTTCGTAAATGGTGA	This study
GFP fusion protein cloning		
mgfp5-FW-*Bam*HI	ATCGATGGATCCATGGCTAGTAAAGGAGAAGAACTTTTC	This study
mgfp5-FW-*Not*I	ATCGATGCGGCCGCATGGCTAGTAAAGGAGAAGAACTTTT	This study
mgfp5-RW-*Kpn*I	ATCGATGGTACCTCATTTGTATAGTTCATCCAT	This study
PT-10k1-RV-*Bam*HI	ATCGATGGATCCTCTAACAAAAAGCATAAGAA	This study
PT-9b13-RV-*Bam*HI	ATGGATCCACGAACAAATTGTATAAGGATG	This study
Ca35S-FW-*Sal*I-2	GATACCGTCGACAAGCTTGCATG	This study
Real time-quantitative PCR		
AHR4DT-1-FW	ACTTCTGGAGTTATACTTGTG	This study
AHR4DT-1-RV	TAGATAGTGATGTGAGGATTATAG	This study
AHR3'DT-1-FW	GCAGCATAATTGGAAGCA	This study
AHR3'DT-1-RV	GGAAAGCATCTAAAGCATCA	This study
JC1-FW	TATGTATTTAACAGAAGAAATAC	(Condori et al., 2009)
JC1-RV	AGTTGCAGCCTCTTTTCCAACT	(Condori et al., 2009)
ACT7-FW	ATGTATGTAGCCATCCAAG	(Condori et al., 2011)
ACT7-RV	ACCAGAGTCCAGAACAATA	(Condori et al., 2011)
EF1α-FW	GGTGTCAAGCAGATGATT	(Condori et al., 2011)
EF1α-RV	ACTTCCTTCACGATTTCA	(Condori et al., 2011)

Table S2. Substrates used for specificity assay and the prenylated products from reaction mixtures catalyzed by AhR4DT-1 or AhR3'DT-1.

Analysis was done by HPLC-PDA-electrospray ionization-MS^3.

No	Analyte	t_R (min)	UV (nm)	$[M+H]^+$ (m/z)	MS^2 ions	MS^3 ions
1	Oxyresveratrol	5.74	243, 302, 328	245	227	**209,** 199, 157
2	Piceatannol	5.79	240, 324	245	227, 199, **135**[a]	107
3	Resveratrol	6.50	237, 306, 317	229	**211**, 183	107
4	Prenylated oxyresveratrol by AhR3'DT-1	9.85	225, 325	313	257	239
5	Prenylated oxyresveratrol by AhR4DT-1	10.63	225, 304, 329	313	257	239
6	Arachidin-5	11.01	240, 327	313	**257**	239, 229, **211**
7	Pinosylvin	12.42	229, 300, 307	213	135	**107**
8	Arachidin-2	13.84	239, 311, 323	297	241	223, 213, **195**
9	Prenylated piceatannol by AhR3'DT-1	14.44	228, 325	313	257	**239,** 211
10	3-methyl-2-butenyl-3'-resveratrol	16.99	230, 320	297	241	223
11	Chiricanine A	25.02	209, 314	281	225	**179**, 207

[a]MS^2 ions in boldface were the most abundant ions and were subjected to MS^3 fragmentation.

Table S3. List of plasmids used in this study.

For details of the binary vectors, see Materials and Methods.

Name	Descirption	Reference
pBC KS(-)	Phagemid vector derived from pBluescript II KS(-)	
pBIB-Kan	Binary vector	(Becker, 1990)
pR8-2	*CaMV35S::TEV::pat::mGFP5* in pBC KS(-)	(Medina-Bolívar and Cramer, 2004)
Prenyltransferase Characterization		
pGEM-CaMV35S-TEV	*CaMV35S::TEV* in pGEM-T	This study
pBC-CaMV35S-TEV-9b13	*CaMV35S::TEV::AhR4DT-1* in pBC KS(-)	This study
pBC-CaMV35S-TEV-10k1	*CaMV35S::TEV::AhR3'DT-1* in pBC KS(-)	This study
pBIB-Kan-AhR4DT-1	*CaMV35S::TEV::AhR4DT-1* in pBIB-Kan	This study
pBIB-Kan-AhR3'DT-1	*CaMV35S::TEV::AhR3'DT-1* in pBIB-Kan	This study
pBIB-Kan-AhR3'DT-2	*CaMV35S::TEV::AhR3'DT-2* in pBIB-Kan	This study
pBIB-Kan-AhR3'DT-3	*CaMV35S::TEV::AhR3'DT-3* in pBIB-Kan	This study
pBIB-Kan-AhR3'DT-4	*CaMV35S::TEV::AhR3'DT-4* in pBIB-Kan	This study
Subcellular Localization		
pt-rk	*CaMV35S::RS-TP-mCherry* in pBIN20	(Nelson et al., 2007)
pGEM-mGFP5-1	*mGFP5* with *Bam*HI/*Kpn*I sites in pGEM-T	This study
pGEM-mGFP5-2	*mGFP5* with *Not*I/*Kpn*I sites in pGEM-T	This study
pGEM-CaMV35S-TEV-AhR4DT-1-GFP	*CaMV35S::TEV::AhR4DT-1::mGFP5* in pGEM-T	This study
pGEM-CaMV35S-TEV-AhR3'DT-1-GFP	*CaMV35S::TEV::AhR3'DT-1::mGFP5* in pGEM-T	This study
pBC-CaMV35S-TEV-GFP	*CaMV35S::TEV::mGFP5* in pBC KS(-)	This study
pBIB-Kan-AhR4DT-1-GFP	*CaMV35S::TEV::AhR4DT-1::mGFP5* in pBIB-Kan	This study
pBIB-Kan-AhR3'DT-1-GFP	*CaMV35S::TEV::AhR3'DT-1::mGFP5* in pBIB-Kan	This study
pBIB-Kan-GFP	*CaMV35S::TEV::mGFP5* in pBIB-Kan	This study

Table S4. Accession numbers of proteins used for phylogenetic analysis.

Protein name	Accession number	Description	Organism
AaVTE2-1	ABB70124.1	homogentisate phytyltransferase VTE2-1	*Allium ampeloprasum*
AhR4DT-1	AQM74172.1	resveratrol-4-dimethylallyltransferase	*Arachis hypogaea*
AhR3'DT-1	AQM74173.1	resveratrol-3'-dimethylallyltransferase	*Arachis hypogaea*
AhR3'DT-2	AQM74174.1	resveratrol-3'-dimethylallyltransferase	*Arachis hypogaea*
AhR3'DT-3	AQM74175.1	resveratrol-3'-dimethylallyltransferase	*Arachis hypogaea*
AhR3'DT-4	AQM74176.1	resveratrol-3'-dimethylallyltransferase	*Arachis hypogaea*
AtHPT1	AAM10489.1	homogentisate phytylprenyltransferase	*Arabidopsis thaliana*
AtPPT1	BAB20818.2	p-hydroxybenzoate polyprenyltransferase	*Arabidopsis thaliana*
AtVTE2-2	ABB70127.1	homogentisate phytyltransferase VTE2-2	*Arabidopsis thaliana*
ClPT1a	BAP27988.1	umbelliferone 8-geranyltransferase	*Citrus limon*
CpVTE2-1	ABB70125.1	homogentisate phytyltransferase VTE2-1	*Cuphea pulcherrima*
CrVTE2-2	CAL01105.1	homogentisate prenyltransferase	*Chlamydomonas reinhardtii*
CtIDT	AJD80983.1	isoliquiritigenin 3'-dimethylallyltransferase	*Cudrania tricuspidata*
GmG4DT	BAH22520.1	pterocarpan 4-dimethylallyltransferase	*Glycine max*
GmVTE2-1	ABB70126.1	homogentisate phytyltransferase VTE2-1	*Glycine max*
GmVTE2-2	ABB70128.1	homogentisate phytyltransferase VTE2-2	*Glycine max*
GuA6DT	AIT11912.1	flavone prenyltransferase	*Glycyrrhiza uralensis*
HlPT-1	BAJ61049.1	aromatic prenyltransferase	*Humulus lupulus*
HvHGGT	AAP43911.1	homogentisic acid geranylgeranyl transferase	*Hordeum vulgare*
LaPT-1	AER35706.1	genistein 3'-dimethylallyltransferase	*Lupinus albus*
LePGT-1	BAB84122.1	4-hydroxybenzoate geranyltransferase	*Lithospermum erythrorhizon*
LePGT-2	BAB84123.1	4-hydroxybenzoate geranyltransferase	*Lithospermum erythrorhizon*
MaIDT	AJD80982.1	isoliquiritigenin 3'-dimethylallyltransferase	*Morus alba*
OsHGGT	AAP43913.1	homogentisic acid geranylgeranyl transferase	*Oryza sativa*
OsPPT1	BAE96574.1	p-hydroxybenzoate polyprenyltransferase	*Oryza sativa*
PcPT	BAO31627.1	umbelliferone 6-dimethylallyltransferase	*Petroselinum crispum*
SfG6DT	BAK52291.1	genistein 6-dimethylallyltransferase	*Sophora flavescens*
SfiLDT	BAK52290.1	isoliquiritigenin dimethylallyltransferase	*Sophora flavescens*
SfN8DT-1	BAG12671.1	naringenin 8-dimethylallyltransferase	*Sophora flavescens*
SfN8DT-2	BAG12673.1	naringenin 8-dimethylallyltransferase	*Sophora flavescens*
SfN8DT-3	BAK52289.1	naringenin 8-dimethylallyltransferase	*Sophora flavescens*
TaHGGT	AAP43912.1	homogentisic acid geranylgeranyl transferase	*Triticum aestivum*
TaVTE2-1	ABB70123.1	homogentisate phytyltransferase VTE2-1	*Triticum aestivum*
ZmVTE2-1	ABB70122.1	homogentisate phytyltransferase VTE2-1	*Zea mays*